

# A Family of Hybrid Federated and Centralized Learning Architectures in Machine Learning

Ahmet M. Elbir, *Senior Member, IEEE*, and Sinem Coleri, *Senior Member, IEEE*

**Abstract**—Many of the machine learning tasks focus on centralized learning (CL), which requires the transmission of local datasets from the clients to a parameter server (PS) entailing huge communication overhead. To overcome this, federated learning (FL) has been a promising tool, wherein the clients send only the model updates to the PS instead of the whole dataset. However, FL demands powerful computational resources from the clients. Therefore, not all the clients can participate in training if they do not have enough computational resources. To address this issue, we introduce a more practical approach called hybrid federated and centralized learning (HFCL), wherein only the clients with sufficient resources employ FL, while the remaining ones send their datasets to the PS, which computes the model on behalf of them. Then, the model parameters corresponding to all clients are aggregated at the PS. To improve the efficiency of dataset transmission, we propose two different techniques: increased computation-per-client and sequential data transmission. The HFCL frameworks outperform FL with up to 20% improvement in the learning accuracy when only half of the clients perform FL while having 50% less communication overhead than CL since all the clients collaborate on the learning process with their datasets.

**Index Terms**—Machine learning, federated learning, centralized learning, edge intelligence, edge efficiency.

## I. INTRODUCTION

The ever growing increase in the number of connected devices in the last few years has led to a surge in the amount of data generated by mobile phones, connected vehicles, drones, internet of things (IoT) devices due to the rapid development of various emerging applications, such as artificial intelligence (AI), virtual and augmented reality (VAR), autonomous vehicles (AVs) and machine-to-machine communications [2, 3]. According to international telecommunication union (ITU), the global mobile traffic is expected to reach 607 EB in 2025 [4]. Moreover, AVs are expected to generate approximately 20 TB/day/vehicle data [5]. In order to process and extract useful information from the huge amount of data, machine learning (ML) has been recognized as a promising tool for several emerging technologies, such as IoT [6], AV [7] and the next generation wireless communications [8–10] due to its success in image/speech recognition, natural language processing, etc [2]. These applications require huge amount of data to be processed and learned by a learning model, often an artificial

neural network (ANN), by extracting the features from the raw data and providing a “meaning” to the input via constructing a model-free data mapping with huge number of learnable parameters [8]. The implementation of these learning models demands powerful computation resources, such as graphics processing units (GPUs). Therefore, huge learning models, massive amount of training data and powerful computation infrastructure are the main driving factors of the success of ML algorithms [3, 8].

Many of the ML tasks focus on centralized learning (CL) algorithms, which train powerful ANNs at a parameter server (PS) [2, 11, 12]. While CL inherently assumes the availability of datasets at the PS, it may not be possible for the wireless edge devices (clients), such as mobile phones, connected vehicles, IoT devices, which need to send their datasets to the PS. Transmitting the collected datasets to the PS in a reliable manner may be too costly in terms of energy, latency and bandwidth [13]. For example, in LTE (long term evolution), a single frame of 5 MHz bandwidth and 10 ms duration can carry only 6000 complex symbols [14], whereas the size of the whole dataset can be on the order of hundreds of thousands symbols [15]. As a result, CL-based techniques demand huge bandwidth and communication overhead during training.

In order to provide a practically viable alternative to CL-based training, federated learning (FL) has been proposed to exploit the processing capability of the edge devices and the local datasets of the clients [12, 16, 17]. In FL, the clients compute and transmit the model parameters to the PS instead of their local datasets as in CL to collaboratively train the learning model. The collected model updates are aggregated at the PS and then broadcast to the clients to further update the learning parameters iteratively. Since FL does not access the whole dataset at once, it has slightly lower learning performance than that of CL. However, FL is communication-efficient and privacy-preserving since it keeps the datasets at the clients. Recently, FL has been applied to image classification [13, 16, 18, 19], speech recognition [20] and wireless communications [21, 22]. In addition, various wireless network architectures exploiting FL have been investigated, such as cellular networks [14, 23, 24], vehicular networks [7], unmanned aerial vehicles [25] and IoT networks [26]. In these works, the FL architectures rely on the fact that all of the clients are capable of model computation, which may require powerful parallel processing units, such as GPUs. However, this may not always be possible in practice due to the diversity of the devices with different computation capabilities, such as mobile phones, vehicular components and IoT devices. When the edge devices suffer from the computational power, they cannot perform model computation, thus become unable to

The work of Sinem Coleri was supported by Ford Otosan and the Scientific and Technological Research Council of Turkey with European CHIST-ERA grant 119E350.

A preliminary work of this paper was presented in 2021 European Signal Processing Conference (EUSIPCO) [1].

Ahmet M. Elbir is with the Department of Electrical and Electronics Engineering, Koc University, Istanbul, Turkey, and with SnT, University of Luxembourg, Luxembourg (e-mail: ahmetmelbir@gmail.com).

Sinem Coleri is with the Department of Electrical and Electronics Engineering, Koc University, Istanbul, Turkey (e-mail: scoleri@ku.edu.tr).

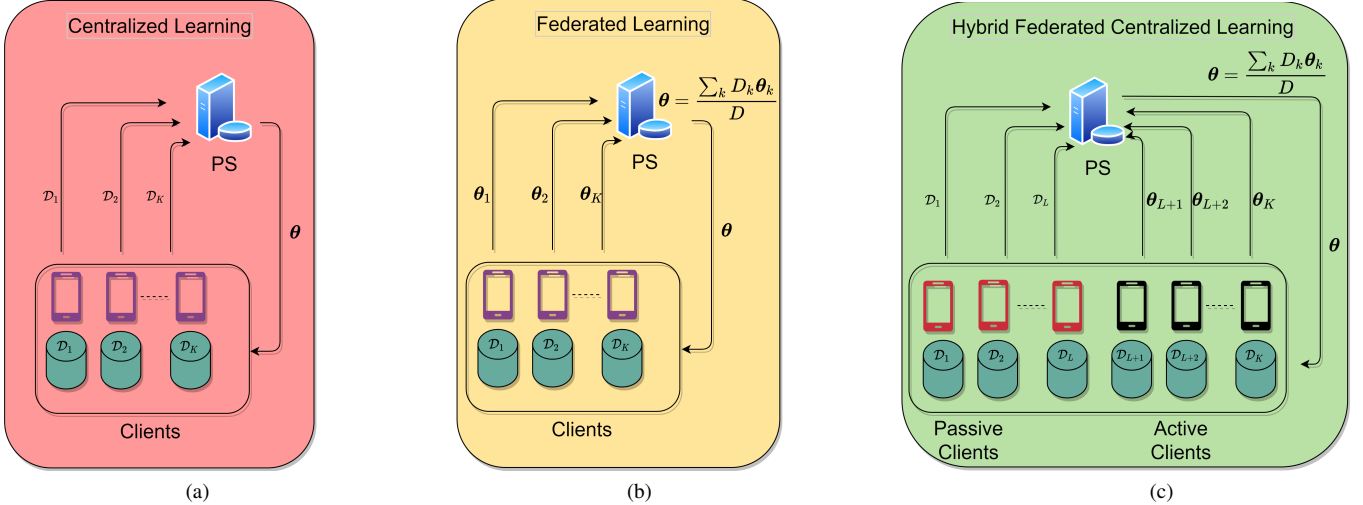


Fig. 1. CL, FL and HFCL frameworks. (a) In CL, all clients transmit their datasets to the PS. (b) In FL, the datasets are preserved at the clients, instead, model parameters are sent to the PS. (c) In HFCL, the clients are designated as active and passive depending on their computational capability to either perform CL or FL.

participate on the learning process. To address this problem, client selection algorithms have been developed. In [27] and [28], trusted clients and the ones with sufficient computational resources are participated in FL-based training, respectively. However, these studies do not allow the clients that are not selected to participate in the training process regardless of their computational capability and the PS to access their dataset.

In this work, we introduce a hybrid FL and CL (HFCL) framework to effectively train a learning model regardless of the computational capability of the clients. By exploiting their computational resources, the clients that are capable of model computation perform FL while the remaining clients resort to CL and send their datasets to the PS, which computes the corresponding model parameters on behalf of them (see Fig. 1). At the beginning of the training, the clients are designated as *passive* (i.e., perform CL) or *active* (i.e., perform FL) depending on their computational capability. That is, the clients are called active if they have adequate computational resources, e.g., GPUs, to compute the model parameters, whereas the clients are called passive otherwise, hence they send their datasets to the PS, which computes the model parameters on behalf of them. During model training, both active and passive clients are synchronized and the training process is conducted iteratively as in FL, where the model parameters are aggregated in each communication round between the PS and the active clients. Prior to the model training, the passive clients transmit the datasets to the PS so that the PS can compute model updates on behalf of them during training. In the meantime, the active clients perform model computation. Once the model parameters corresponding to active (computed on device) and passive (computed on PS) clients are collected at the PS, they are aggregated and broadcast to the active clients only so that they can compute the model parameters in the next iteration. Since the PS computes the model parameters on behalf of the passive clients, it is not necessary to broadcast model updates to them.

A challenging issue in HFCL is that the active clients should wait for the passive clients at the beginning of the training until the dataset transmission for passive clients is completed so that they can synchronously participate on model training. To circumvent this problem and provide efficient model training, we propose two approaches, i.e., sequential dataset transmission (HFCL-SDT) and increased computation-per-client (HFCL-ICpC). In HFCL-ICpC approach, the training continues at the active clients during the transmission of passive clients' datasets instead of waiting idle for the passive clients as in HFCL, in which the active clients wait for the completion of dataset transmission. Thus, HFCL-ICpC improves the learning performance as compared to HFCL without increasing the delay due to dataset generation. This delay is reduced in HFCL-SDT approach by dividing the passive clients' datasets into smaller blocks so that the dataset transmission is completed quicker than HFCL and HFCL-ICpC. In summary, HFCL-ICpC improves learning performance while HFCL-SDT reduces the dataset transmission time per communication round. Inspired from [16], where the model parameters are infrequently aggregated at the clients, we develop a new approach to first aggregate the model parameters at the clients until the transmission of the passive clients' datasets is completed, then continue aggregating the models at the PS. Compared to [16], our technique has better learning performance as well as flexibility on the hardware requirements since the learning model can be trained on the whole dataset even if a part of the clients do not have computational resources. Compared to our preliminary work [1], this introduces HFCL-ICpC approach to improve learning accuracy, theoretical analysis on the convergence of HFCL, and the implementation of the 3-D object detection scenario. The main contributions of this paper are as follows:

- We propose a hybrid FL/CL approach to take into account the computational capability of the edge clients. In the proposed approach, only the clients which have adequate

TABLE I  
COMPARISON OF CL, FL AND HFCL

Property \ Framework	CL	FL	HFCL
Communication Overhead	High	Low	Moderate
Learning Accuracy	High	Moderate	Moderate
Clients' Hardware Requirement	Low	High	Flexible
Privacy-Preserving	Low	High	Moderate

computational resources perform FL while the remaining clients perform CL. To the best of our knowledge, this is the first work to employ a hybrid architecture exploiting the hardware capability of the edge devices.

- The proposed HFCL approach provides a trade-off for learning performance, communication overhead, privacy and the clients' computational resources (see, e.g., Table I). While the usage of CL enables higher learning performance and less dependence on the clients' computational resources, FL enjoys enhanced privacy and less communication overhead. HFCL jointly employs CL and FL, therefore, it enjoys less communication overhead than CL; higher performance and more flexibility than FL, while it is less privacy-preserving and less communication-efficient than FL.
- We show that the performance of HFCL converges to that of FL (CL) when the number of active clients increases (decreases). Specifically when the active and passive clients are partitioned equally, the proposed HFCL approach exhibits up to 20% improvement in the learning accuracy as compared to FL. HFCL also enjoys 50% less communication overhead with only 2% loss in the learning accuracy as compared to CL.
- In order to efficiently transmit the datasets of the passive clients to the PS, we propose SDT and ICpC techniques so that the learning process is not interrupted. Compared to FL, the proposed techniques are effective due to faster convergence rates and higher learning accuracy and less communication delay due to dataset transmission.

*Notation:* Throughout the paper, the identity matrix of size  $N \times N$  is denoted by  $\mathbf{I}_N$ .  $(\cdot)^T$  denotes transpose operation. For a matrix  $\mathbf{A}$  and a vector  $\mathbf{a}$ ,  $[\mathbf{A}]_{i,j}$  and  $[\mathbf{a}]_i$  denote the  $(i,j)$ th element of matrix  $\mathbf{A}$  and the  $i$ th element of vector  $\mathbf{a}$ , respectively. The function  $\mathbb{E}\{\cdot\}$  provides the statistical expectation of its argument.  $\|\mathbf{a}\|$  denote the  $l_2$ -norm and  $\nabla$  represents the gradient of vector quantity. A convolutional layer with  $N \times D \times D$  2-D kernel is represented by  $N @ D \times D$ .

The rest of the paper is organized as follows. In Section II, CL and FL frameworks are presented. Then, we introduce the proposed HFCL, HFCL-ICpC and HFCL-SDT approach in Section III, IV and V. We investigate the convergence and the communication overhead of the HFCL approach in Section VI. Section VII presents the numerical simulation results and we summarize the paper in Section VIII with concluding remarks.

## II. PRELIMINARIES:

## CENTRALIZED AND FEDERATED LEARNING

In ML, we are interested in constructing a learning model that forms a non-linear relationship between the two data pairs: input and the label. Let  $\mathcal{D}^{(i)} = (\mathcal{X}^{(i)}, \mathcal{Y}^{(i)})$  be the  $i$ th tuple of the dataset  $\mathcal{D}$  for  $i = 1, 2, \dots, D$ , where  $D = |\mathcal{D}|$  denotes the number of data instances in  $\mathcal{D}$ . Here,  $\mathcal{X}^{(i)} \in \mathbb{R}^{U_x \times V_x}$  and  $\mathcal{Y}^{(i)} \in \mathbb{R}^{U_y \times V_y}$  denote the  $i$ th input and the label pairs of  $\mathcal{D}$ , respectively. Then, the non-linear function representing the ML model can be given by  $f(\mathcal{X}^{(i)}|\boldsymbol{\theta}) = \mathcal{Y}^{(i)}$ , for which  $\boldsymbol{\theta} \in \mathbb{R}^P$  denotes the vector of learnable model parameters. In order to train the ML model, we focus on a scenario, wherein  $K$  clients collaborate on optimizing  $\boldsymbol{\theta}$  for the ML task.

### A. Centralized Learning

In CL, the model has access to the whole dataset  $\mathcal{D}$ , which can be collected at the PS from the clients (see Fig. 1a). Let  $\mathcal{D}_k$  be the local dataset of the  $k$ th client with  $D_k$  being the size of the local dataset such that  $\mathcal{D} = \bigcup_{k \in \mathcal{K}} \mathcal{D}_k$  and  $D = \sum_{k \in \mathcal{K}} D_k$ , where  $\mathcal{K} = \{1, \dots, K\}$ . Then, the CL-based model training can be performed at the PS by solving

$$\min_{\boldsymbol{\theta}} \mathcal{F}(\boldsymbol{\theta}) = \sum_{k=1}^K \frac{D_k}{D} \mathcal{F}_k(\boldsymbol{\theta}),$$

$$\text{subject to: } f(\mathcal{X}_k^{(i)}|\boldsymbol{\theta}) = \mathcal{Y}_k^{(i)}, \quad i = 1, \dots, D_k, \quad (1)$$

where  $\mathcal{X}_k^{(i)}$  and  $\mathcal{Y}_k^{(i)}$  respectively denote the input and output of the  $i$ th element of  $\mathcal{D}_k$  as  $\mathcal{D}_k^{(i)} = (\mathcal{X}_k^{(i)}, \mathcal{Y}_k^{(i)})$ .  $\mathcal{F}_k(\boldsymbol{\theta})$  is the loss function over  $\boldsymbol{\theta}$ , and it can be defined for regression and classification tasks, respectively, as

$$\mathcal{F}_k(\boldsymbol{\theta}) = \frac{1}{D_k} \sum_{i=1}^{D_k} \|f(\mathcal{X}_k^{(i)}|\boldsymbol{\theta}) - \mathcal{Y}_k^{(i)}\|^2, \quad (2)$$

and

$$\begin{aligned} \mathcal{F}_k(\boldsymbol{\theta}) = & -\frac{1}{D_k} \sum_{i=1}^{D_k} [\mathcal{Y}_k^{(i)} \ln f(\mathcal{X}_k^{(i)}|\boldsymbol{\theta}) \\ & + (1 - \mathcal{Y}_k^{(i)}) \ln(1 - f(\mathcal{X}_k^{(i)}|\boldsymbol{\theta}))]. \end{aligned} \quad (3)$$

### B. Federated Learning

Compared to CL, FL does not involve the transmission of datasets to the PS. Instead, the model training is performed at the clients while the model parameters produced by the clients are aggregated at the PS, as shown in Fig. 1b. Consequently, the optimization problem in (1) is solved as

$$\text{Client : } \boldsymbol{\theta}_k = \arg \min_{\boldsymbol{\theta}} \mathcal{F}_k(\boldsymbol{\theta}), \quad k \in \mathcal{K}, \quad (4a)$$

$$\text{PS : } \boldsymbol{\theta} = \frac{\sum_{k \in \mathcal{K}} D_k \boldsymbol{\theta}_k}{D}, \quad (4b)$$

in which each client optimizes its model parameters  $\boldsymbol{\theta}_k$  based on  $\mathcal{F}_k(\boldsymbol{\theta})$  as in (4a) and transmits  $\boldsymbol{\theta}_k$  to the PS, where the the model parameters are aggregated as in (4b). In order to solve (4a) effectively, gradient descent (GD) algorithm is used iteratively such that an optimal local solution is obtained for each iteration. The PS and the clients exchange the updated

model parameters until convergence [12, 16, 29]. In particular, the parameter update at the  $t$ th iteration is performed as

$$\boldsymbol{\theta}_k^{(t+1)} = \boldsymbol{\theta}_k^{(t)} - \eta \mathbf{g}(\boldsymbol{\theta}_k^{(t)}), \quad (5)$$

where  $\boldsymbol{\theta}_k^{(t)}$  denotes the model parameters at the  $k$ th client for the  $t$ th communication round/iteration with  $t = 1, \dots, T$  for total number of iterations  $T$ ,  $\eta$  is the learning rate and  $\mathbf{g}(\boldsymbol{\theta}_k^{(t)}) = \nabla \mathcal{F}_k(\boldsymbol{\theta}_k^{(t)})$  denotes the  $P \times 1$  gradient vector, computed at the  $k$ th client, based on  $\mathcal{D}_k$  and  $\boldsymbol{\theta}_k^{(t)}$ . Then, we can rewrite (4) as

$$\text{Client : } \boldsymbol{\theta}_k^{(t+1)} = \boldsymbol{\theta}_k^{(t)} - \eta \mathbf{g}(\boldsymbol{\theta}_k^{(t)}), \quad k \in \mathcal{K}, \quad (6a)$$

$$\text{PS : } \boldsymbol{\theta}^{(t+1)} = \frac{\sum_{k \in \mathcal{K}} D_k \boldsymbol{\theta}_k^{(t+1)}}{D}, \quad (6b)$$

which performs GD and iteratively reaches to the convergence.

### III. HYBRID FEDERATED AND CENTRALIZED LEARNING

In this section, we introduce the proposed HFCL framework by taking into account the computational capability of the clients so that all of the clients can contribute to the learning task with their datasets regardless of their ability to compute model parameters. In ML tasks, training a model requires huge computational power to compute the model parameters. This requirement cannot always be satisfied by the computational capability of the client devices. In order to train the ML model effectively taking into account the computational capability of the clients, a hybrid training framework is introduced in this work. We assume that only a portion of the clients with sufficient computational power performs FL, while the remaining clients, which suffer from computational capability, send their datasets to the PS for model computation, as illustrated in Fig. 1c.

Let us define the set of clients who perform CL, i.e., sending datasets to the PS, and the ones who perform FL, i.e., transmitting the model parameters to the PS as  $\mathcal{L} = \{1, \dots, L\}$  and  $\bar{\mathcal{L}} = \{L+1, \dots, K\}$ , respectively, where  $\mathcal{K} = \mathcal{L} \cup \bar{\mathcal{L}}$  and  $\mathcal{L} \cap \bar{\mathcal{L}} = \emptyset$ . Furthermore, we refer to the clients in  $\mathcal{L}$  and  $\bar{\mathcal{L}}$  as *passive* and *active* clients, respectively. By exploiting the availability of computational resources of the clients, the HFCL problem can be formulated as

$$\text{Client : } \boldsymbol{\theta}_k = \arg \min_{\boldsymbol{\theta}} \mathcal{F}_k(\boldsymbol{\theta}), \quad k \in \bar{\mathcal{L}}, \quad (7a)$$

$$\text{PS : } \boldsymbol{\theta}_k = \arg \min_{\boldsymbol{\theta}} \mathcal{F}_k(\boldsymbol{\theta}), \quad k \in \mathcal{L}, \quad (7b)$$

$$\text{PS : } \boldsymbol{\theta} = \frac{\sum_{k \in \mathcal{K}} D_k \boldsymbol{\theta}_k}{D}, \quad (7c)$$

where the PS actively participates in the model computation process and computes  $\boldsymbol{\theta}_k$  for  $k \in \mathcal{L}$ , then aggregates the model parameters as in (7c).

#### A. Noisy Learning Model

During model transmission for  $k \in \bar{\mathcal{L}}$ , the model parameters are corrupted by noise due to the wireless links [21, 22, 29].

Then, the noisy model parameters at the PS and the clients are respectively given by

$$\text{Client : } \tilde{\boldsymbol{\theta}}_k = \tilde{\boldsymbol{\theta}} + \Delta \tilde{\boldsymbol{\theta}}_k, \quad k \in \bar{\mathcal{L}}, \quad (8a)$$

$$\text{PS : } \tilde{\boldsymbol{\theta}} = \frac{1}{D} \left\{ \sum_{k \in \mathcal{L}} D_k \boldsymbol{\theta}_k + \sum_{k \in \bar{\mathcal{L}}} D_k (\boldsymbol{\theta}_k + \Delta \boldsymbol{\theta}_k) \right\}. \quad (8b)$$

In (8b),  $\boldsymbol{\theta}_{k \in \bar{\mathcal{L}}}$  denotes the true model parameter transmitted from the active clients while  $\Delta \boldsymbol{\theta}_{k \in \bar{\mathcal{L}}}$  represents the noise term added onto  $\boldsymbol{\theta}_{k \in \bar{\mathcal{L}}}$  captured at the PS. After model aggregation in (8b),  $\tilde{\boldsymbol{\theta}}$  is broadcast to the active clients and it is corrupted by the noise term  $\Delta \tilde{\boldsymbol{\theta}}_k$  as in (8a) for  $k \in \bar{\mathcal{L}}$ . Notice that the first term on the right hand side of (8b) includes no noise corruption since the model parameters are computed at the PS. Let us rewrite (8b) as

$$\tilde{\boldsymbol{\theta}} = \frac{1}{D} \sum_{k \in \mathcal{K}} D_k \boldsymbol{\theta}_k + \frac{1}{D} \sum_{k \in \bar{\mathcal{L}}} D_k \Delta \boldsymbol{\theta}_k. \quad (9)$$

Then, using (4b), (9) becomes

$$\tilde{\boldsymbol{\theta}} = \boldsymbol{\theta} + \tilde{\Delta \boldsymbol{\theta}}, \quad (10)$$

where  $\tilde{\Delta \boldsymbol{\theta}} = \frac{1}{D} \sum_{k \in \bar{\mathcal{L}}} D_k \Delta \boldsymbol{\theta}_k$  is the aggregated noise term due to the model transmission from the active clients to the PS. Without loss of generality, we assume that both noise terms due to model transmission in client-PS and PS-client links, i.e.,  $\tilde{\Delta \boldsymbol{\theta}}$  and  $\Delta \tilde{\boldsymbol{\theta}}_k$  ( $k \in \bar{\mathcal{L}}$ ), are additive white Gaussian noise (AWGN) vectors [22, 29]. Hence, for the aggregation noise at the PS, we have  $\mathbb{E}\{\tilde{\Delta \boldsymbol{\theta}}\} = \mathbf{0}$  and  $\mathbb{E}\{\tilde{\Delta \boldsymbol{\theta}} \tilde{\Delta \boldsymbol{\theta}}^\top\} = \tilde{\sigma}^2 \mathbf{I}_P$ . Likewise, at the  $k$ th active client ( $k \in \bar{\mathcal{L}}$ ), we have  $\mathbb{E}\{\Delta \tilde{\boldsymbol{\theta}}_k\} = \mathbf{0}$ ,  $\mathbb{E}\{\Delta \tilde{\boldsymbol{\theta}}_k \Delta \tilde{\boldsymbol{\theta}}_k^\top\} = \sigma_k^2 \mathbf{I}_P$  and  $\mathbb{E}\{\Delta \tilde{\boldsymbol{\theta}}_{k_1} \Delta \tilde{\boldsymbol{\theta}}_{k_2}^\top\} = \mathbf{0}$  for  $k_1, k_2 \in \bar{\mathcal{L}}$  and  $k_1 \neq k_2$ . Furthermore, by using (10) and rewriting (8a) as

$$\tilde{\boldsymbol{\theta}}_k = \boldsymbol{\theta} + \tilde{\Delta \boldsymbol{\theta}} + \Delta \tilde{\boldsymbol{\theta}}_k = \boldsymbol{\theta} + \tilde{\Delta \boldsymbol{\theta}}_k, \quad (11)$$

we can define the noise on  $\boldsymbol{\theta}$  at the  $k$ th client with variance  $\tilde{\sigma}^2 + \sigma_k^2$ . Specifically,  $\tilde{\sigma}^2$  is due to the noise term  $\tilde{\Delta \boldsymbol{\theta}}$  in (10) generated during the model transmission from active clients to the PS while  $\sigma_k^2$  corresponds to  $\tilde{\Delta \boldsymbol{\theta}}_k$  in (11) which is due to the transmission of the model parameters from the PS to the  $k$ th active client.

Upon the above analysis on the noise corruption, it is clear that two different noise corruptions occur during training: noise corruption with  $\tilde{\sigma}^2$  and  $\tilde{\sigma}^2 + \sigma_k^2$  for passive and active clients, respectively. In the sequel, we modify the loss functions used in the training process according to the noise corruption to provide an expectation-based convergence [16, 19].

Let us first consider the loss function for active clients to solve (7a). In order to solve the local problem in (7a) effectively, the loss function should be modified to take into account the effect of noise. Thus, we define a regularized loss function  $\bar{\mathcal{F}}_k(\boldsymbol{\theta})$  as

$$\bar{\mathcal{F}}_k(\boldsymbol{\theta}) = \mathcal{F}_k(\boldsymbol{\theta}) + (\tilde{\sigma}^2 + \sigma_k^2) \|\mathbf{g}(\boldsymbol{\theta}_k)\|^2, \quad (12)$$

where  $\tilde{\sigma}^2 + \sigma_k^2$  corresponds to the total noise term added onto  $\boldsymbol{\theta}$  at the  $k$ th client ( $k \in \bar{\mathcal{L}}$ ) in (11). The loss function in (12) is widely used in stochastic optimization [30] and it can be

obtained via first order Taylor expansion of the expectation-based loss  $\mathbb{E}\{\|\mathcal{F}_k(\boldsymbol{\theta} + \widehat{\Delta}\boldsymbol{\theta}_k)\|^2\}$ , which can be approximately written as

$$\begin{aligned} \mathbb{E}\{\|\mathcal{F}_k(\boldsymbol{\theta} + \widetilde{\Delta}\boldsymbol{\theta}_k)\|^2\} &\approx \mathbb{E}\{\|\mathcal{F}_k(\boldsymbol{\theta}) + \widetilde{\Delta}\boldsymbol{\theta}_k \nabla \mathcal{F}_k(\boldsymbol{\theta})\|^2\}, \\ &\approx \mathbb{E}\{\|\mathcal{F}_k(\boldsymbol{\theta})\|^2\} + \mathbb{E}\{\|\widetilde{\Delta}\boldsymbol{\theta}_k\|^2\} \mathbb{E}\{\|\nabla \mathcal{F}_k(\boldsymbol{\theta})\|^2\}, \\ &\approx \mathbb{E}\{\|\mathcal{F}_k(\boldsymbol{\theta})\|^2\} + (\tilde{\sigma}^2 + \sigma_k^2) \|\mathbf{g}(\boldsymbol{\theta}_k)\|^2, \end{aligned} \quad (13)$$

where the first term corresponds to the minimization of the loss function with perfect estimation and the second term is the additional cost due to noise. The expectation-based loss in (13) provides a good approximation under the effect of uncertainties due to the noise by adding the regularizer term  $(\tilde{\sigma}^2 + \sigma_k^2) \|\mathbf{g}(\boldsymbol{\theta}_k)\|^2$  [29, 30]. Similarly, the loss function in (7b) for passive clients at the PS can be regularized as

$$\tilde{\mathcal{F}}_k(\boldsymbol{\theta}) = \mathcal{F}_k(\boldsymbol{\theta}) + \tilde{\sigma}^2 \|\mathbf{g}(\boldsymbol{\theta}_k)\|^2. \quad (14)$$

Combining (8b), (12) and (14) yields the regularized version of the HFCL problem as

$$\text{Client : } \boldsymbol{\theta}_k = \arg \min_{\boldsymbol{\theta}} \tilde{\mathcal{F}}_k(\boldsymbol{\theta}), \quad k \in \bar{\mathcal{L}}, \quad (15a)$$

$$\text{PS : } \boldsymbol{\theta}_k = \arg \min_{\boldsymbol{\theta}} \tilde{\mathcal{F}}_k(\boldsymbol{\theta}), \quad k \in \mathcal{L}, \quad (15b)$$

$$\text{PS : } \tilde{\boldsymbol{\theta}} = \frac{1}{D} \left\{ \sum_{k \in \mathcal{L}} D_k \boldsymbol{\theta}_k + \sum_{k \in \bar{\mathcal{L}}} D_k (\boldsymbol{\theta}_k + \Delta \boldsymbol{\theta}_k) \right\}, \quad (15c)$$

where the training on the active and passive clients are performed in (15a) and (15b), respectively. To effectively solve (15), the GD algorithm is utilized to find an optimal model  $\boldsymbol{\theta}$  for all clients, then the model parameter update is performed iteratively as follows

$$\text{Client : } \boldsymbol{\theta}_k^{(t+1)} = \boldsymbol{\theta}_k^{(t)} - \eta \bar{\mathbf{g}}_k(\boldsymbol{\theta}_k^{(t)}), \quad k \in \bar{\mathcal{L}}, \quad (16a)$$

$$\text{PS : } \boldsymbol{\theta}_k^{(t+1)} = \boldsymbol{\theta}_k^{(t)} - \eta \tilde{\mathbf{g}}_k(\boldsymbol{\theta}_k^{(t)}), \quad k \in \mathcal{L}, \quad (16b)$$

$$\text{PS : } \tilde{\boldsymbol{\theta}}^{(t+1)} = \frac{1}{D} \sum_{k \in \mathcal{K}} D_k \boldsymbol{\theta}_k^{(t+1)}, \quad (16c)$$

where  $\bar{\mathbf{g}}_k(\boldsymbol{\theta}_k^{(t)}) = \nabla \tilde{\mathcal{F}}_k(\boldsymbol{\theta}_k^{(t)})$  and  $\tilde{\mathbf{g}}_k(\boldsymbol{\theta}_k^{(t)}) = \nabla \mathcal{F}_k(\boldsymbol{\theta}_k^{(t)})$  denote the gradient of the regularized loss function in (12) and (14), respectively. In (16), (16a) and (16b) compute the parameter updates for active and passive clients, respectively. Then, the model aggregation is performed at the PS as in (16c) and the aggregated model  $\tilde{\boldsymbol{\theta}}^{(t+1)}$  is broadcast to the active clients.

### B. Communication Delay During Model Training

The bandwidth resources need to be optimized to reduce the latency of the transmission of both  $\boldsymbol{\theta}_k$  ( $k \in \bar{\mathcal{L}}$ ) and  $\mathcal{D}_k$  ( $k \in \mathcal{L}$ ) to the PS during training. Let  $\tau_k$  be the communication time for the  $k$ th client to transmit its either dataset ( $\mathcal{D}_k$  for  $k \in \mathcal{L}$ ) or model parameters ( $\boldsymbol{\theta}_k$  for  $k \in \bar{\mathcal{L}}$ ), and can be defined as

$$\tau_k = \frac{d_k}{R_k}, \quad (17)$$

where  $d_k$  denotes the number of dataset symbols to transmit and  $R_k = B_k \ln(1 + \text{SNR}_k)$  is the achievable transmission

rate, for which  $B_k$  and  $\text{SNR}_k$ , respectively, denote the allocated bandwidth and the signal-to-noise ratio (SNR) for the  $k$ th client. The PS solves  $\min_{B_k} \max_{k \in \mathcal{K}} \tau_k$  to optimize the bandwidth allocation by minimizing the maximum communication delay. This is because the model aggregation in the PS can be performed only after the completion of the slowest transmission for  $k \in \mathcal{K}$ . Although  $R_k$  can vary for  $k \in \mathcal{K}$ ,  $d_k$  differentiates more significantly than  $R_k$  between the passive (i.e.,  $k \in \mathcal{L}$ ) and active (i.e.,  $k \in \bar{\mathcal{L}}$ ) clients [31]. Depending on the client type,  $d_k$  can be given by

$$d_k = \begin{cases} P, & k \in \bar{\mathcal{L}} \\ \mathbf{d}_k, & k \in \mathcal{L} \end{cases}, \quad (18)$$

which is fixed to the number of model parameters  $P$  for the active clients and to  $\mathbf{d}_k = D_k(U_x V_x + U_y V_y)$  for  $D_k$  input ( $\in \mathbb{R}^{U_x \times V_x}$ ) and output ( $\in \mathbb{R}^{U_y \times V_y}$ ) dataset samples.

Since the dataset size is usually larger than the number of model parameters in ML applications, i.e.,  $\mathbf{d}_{k \in \mathcal{L}} > P$  [12, 13, 21], the dataset transmission of the passive clients is expected to take longer than the model transmission of the active clients, i.e.,  $\tau_{k \in \mathcal{L}} > \tau_{k \in \bar{\mathcal{L}}}$  [31]. Previous FL-based works reported that  $\tau_{k \in \mathcal{L}}$  can be approximately 10 times longer than  $\tau_{k \in \bar{\mathcal{L}}}$  [21, 22]. This introduces a significant delay especially at the beginning of the training since the HFCL problem in (15b) or (16b) can be performed only if  $\mathcal{D}_{k \in \mathcal{L}}$  is collected at the PS for the first iteration. To circumvent this issue and keep the training continue, in the following, we propose two approaches ICpC and SDT in Section IV and V, respectively. Both of these techniques work only at the beginning of the training so that the dataset transmission of the passive clients can be handled effectively.

### IV. HFCL WITH INCREASED COMPUTATION-PER-CLIENT

Prior to the model training, i.e.,  $t = 0$ , the active clients need to wait until the passive clients complete the dataset transmission, during which the active clients perform only one model computation. In order to keep the active clients continue model computing during the data transmission of passive clients, we propose ICpC approach, wherein the active clients move forward computing local model updates, but do not send them to the PS until the dataset transmission of the passive clients is completed. This approach improves the convergence rate and the learning performance due to the continuation of the model updates at the passive clients as similar observations are also reported in [16], in which FL-only training is presented.

The algorithmic steps of HFCL-ICpC approach are presented in Algorithm 1, for which the inputs are the datasets  $\mathcal{D}_{k \in \mathcal{K}}$  and the learning rate  $\eta$ . Different from HFCL, HFCL-ICpC involves the model updates at the active clients during first communication round, i.e.,  $t = 0$ , as in the line 6 – 9 of Algorithm 1. Using (17) and (18), and defining  $Q$  as the block size, the active clients can perform  $N = \frac{\max_{k \in \mathcal{L}} \mathbf{d}_k}{Q}$  iterations when  $t = 0$  until the dataset transmission of the passive clients is completed (Line 10 of Algorithm 1). Although this method keeps the active clients busy with model computation instead of staying idle, it does not reduce the communication latency at the first iteration. As a result, the active clients perform  $N$

**Algorithm 1 HFCL-ICpC**


---

**Input:**  $\eta, \mathcal{D}_{k \in \mathcal{K}}$ .  
**Output:**  $\theta$ .

- 1: Initialize with  $\theta_k^{(t)}$  for  $t = 0$ .
- 2: **repeat**
- 3:     **if**  $k \in \bar{\mathcal{L}}$  [Active clients],
- 4:         **if**  $t = 0$
- 5:              $t' := t$ .
- 6:             **repeat**
- 7:                  $\theta_k^{(t'+1)} = \theta_k^{(t')} - \eta \bar{\mathbf{g}}_k(\theta_k^{(t')})$ .
- 8:                  $t' \leftarrow t' + 1$ .
- 9:             **until**  $t' = N$
- 10:              $\theta_k^{(t+1)} = \theta_k^{(N)}$ .
- 11:         **else**
- 12:              $\theta_k^{(t+1)} = \theta_k^{(t)} - \eta \bar{\mathbf{g}}_k(\theta_k^{(t)})$ .
- 13:         **end**
- 14:         Send  $\theta_k^{(t+1)}$  to the PS.
- 15:     **if**  $k \in \mathcal{L}$  [Passive clients],
- 16:         **if**  $t = 0$
- 17:             Send  $\mathcal{D}_k$  to the PS.
- 18:         **else**
- 19:              $\theta_k^{(t+1)} = \theta_k^{(t)} - \eta \tilde{\mathbf{g}}_k(\theta_k^{(t)})$ .
- 20:         **end**
- 21:     **end**
- 22:     Aggregate models as  $\theta^{(t+1)} = \frac{1}{D} \sum_{k \in \mathcal{K}} D_k \theta_k^{(t+1)}$ .
- 23:     Broadcast  $\theta^{(t+1)}$  to the clients for  $k \in \bar{\mathcal{L}}$ .
- 24:      $t \leftarrow t + 1$ .
- 25: **until** convergence

---

local updates, which improve the convergence rate from  $O(\frac{1}{t})$  to  $O(\frac{N^2}{t})$  as compared to HFCL [32].

## V. HFCL WITH SEQUENTIAL DATA TRANSMISSION

Compared to HFCL and HFCL-ICpC, wherein the first communication round awaits the completion of the transmission of passive clients' datasets  $\mathcal{D}_{k \in \mathcal{L}}$ , HFCL-SDT involves the transmission of smaller blocks of datasets so that the data transmission time per communication round is smaller while the total amount of time to transmit  $\mathcal{D}_{k \in \mathcal{L}}$  to the PS is the same as in HFCL and HFCL-ICpC.

The algorithmic steps of HFCL-SDT approach are given in Algorithm 2. Let  $Q$  be the block size of each portion. The number of blocks can be calculated as  $N = \frac{\max_{k \in \mathcal{L}} \mathbf{d}_k}{Q}$ , which aims to minimize the latency when  $t = 0$  by taking into account the largest dataset with  $\max_{k \in \mathcal{L}} \mathbf{d}_k$  since we need to wait until the transmission of the largest dataset. If  $\mathbf{d}_{k_1} = \mathbf{d}_{k_2}$  for  $k_1, k_2 \in \mathcal{L}$ , then the size of the transmitted data for all clients becomes the same and equals to  $Q$ <sup>1</sup>. If  $N$  is not an integer, then  $N = \lceil \frac{\max_{k \in \mathcal{L}} \mathbf{d}_k}{Q} \rceil$  can be selected. Let us assume that  $\mathcal{F}_k(\theta)$  is the regression loss as in (2)<sup>2</sup>, then, the loss

<sup>1</sup>As a special case,  $Q = P$  can be selected so that the transmitted data from both passive and active clients can be equal. However, this is only possible if  $N = \frac{\max_{k \in \mathcal{L}} \mathbf{d}_k}{P} < \gamma T$  so that dataset transmission is completed before  $\gamma T$  iterations. If  $\gamma = 1$ , then both dataset transmission and the training are completed at the same time, which is not efficient. Empirically,  $\gamma = 0.1$  is a good choice.

<sup>2</sup>The same expression can also be written for the loss function in (3).

**Algorithm 2 HFCL-SDT**


---

**Input:**  $\eta, \mathcal{D}_{k \in \mathcal{K}}, \mathcal{F}_k$  as in (2).  
**Output:**  $\theta$ .

- 1: Initialize with  $\theta_k^{(t)}$  for  $t = 0$ .
- 2: **repeat**
- 3:     **if**  $k \in \bar{\mathcal{L}}$  [Active clients],
- 4:          $\theta_k^{(t+1)} = \theta_k^{(t)} - \eta \bar{\mathbf{g}}_k(\theta_k^{(t)})$ .
- 5:         Send  $\theta_k^{(t+1)}$  to the PS.
- 6:     **if**  $k \in \mathcal{L}$  [Passive clients],
- 7:         **if**  $t \leq N$
- 8:             Send  $\mathcal{D}_k^{(i)}$  to the PS for  $i = (t-1)Q+1, \dots, tQ$ .
- 9:             Use the collected dataset and compute
- 10:              $\mathcal{F}_k(\theta_k^{(t)}) = \frac{\sum_{i=1}^{tQ} \|f(\mathcal{X}_k^{(i)} | \theta_k^{(t)}) - \mathcal{Y}_k^{(i)}\|^2}{tQ}$ .
- 11:             **if**  $t > N$
- 12:                 Use the whole dataset and compute
- 13:                  $\mathcal{F}_k(\theta_k^{(t)}) = \frac{\sum_{i=1}^{D_k} \|f(\mathcal{X}_k^{(i)} | \theta_k^{(t)}) - \mathcal{Y}_k^{(i)}\|^2}{D_k}$ .
- 14:             **end**
- 15:              $\theta_k^{(t+1)} = \theta_k^{(t)} - \eta \tilde{\mathbf{g}}_k(\theta_k^{(t)})$ .
- 16:         **end**
- 17:         Aggregate models as  $\theta^{(t+1)} = \frac{1}{D} \sum_{k \in \mathcal{K}} D_k \theta_k^{(t+1)}$ .
- 18:         Broadcast  $\theta^{(t+1)}$  to the clients for  $k \in \bar{\mathcal{L}}$ .
- 19:          $t \leftarrow t + 1$ .
- 20: **until** convergence

---

function for the passive clients are computed for the HFCL-SDT algorithm as

$$\mathcal{F}_k(\theta_k^{(t)}) = \begin{cases} \frac{\sum_{i=1}^{tQ} \|f(\mathcal{X}_k^{(i)} | \theta_k^{(t)}) - \mathcal{Y}_k^{(i)}\|^2}{tQ}, & t \leq N \\ \frac{\sum_{i=1}^{D_k} \|f(\mathcal{X}_k^{(i)} | \theta_k^{(t)}) - \mathcal{Y}_k^{(i)}\|^2}{D_k}, & t > N \end{cases}, \quad (19)$$

as given in line 6–14 of Algorithm 2. The size of the training dataset collected at the PS (i.e.,  $tQ$ ) for  $\mathcal{F}_k(\theta_k^{(t)})$  becomes larger as  $t \rightarrow N$  and becomes equal to  $D_k$  when  $t = N$ . When  $t > N$ ,  $\mathcal{F}_k(\theta_k^{(t)})$  is computed for the whole dataset of passive clients for  $k \in \mathcal{L}$ , as in the 11th step of Algorithm 2. While the size of the transmitted data from the passive clients changes, the size of the transmitted information is fixed as  $P$  for the active clients. This approach not only reduces the latency of the passive clients, but also improves the learning accuracy as compared to HFCL since the features in the data are quickly learned at the PS due to the use of smaller datasets at the beginning. As a result, the model parameters corresponding to the passive clients are computed as in mini-batch learning case, in which the dataset is partitioned into mini-batches of size  $Q$ . Thus, the convergence rate of the passive clients in HFCL-SDT is  $O(\frac{1}{\sqrt{Q}t} + \frac{1}{t})$  while the active clients have the rate  $O(\frac{1}{t})$  [33].

## VI. CONVERGENCE ANALYSIS AND COMMUNICATION OVERHEAD

In this section, we investigate the efficiency of the proposed HFCL framework in terms of the convergence and communication overhead.

TABLE II  
CONVERGENCE RATES FOR HFCL, HFCL-ICpC AND HFCL-SDT

HFCL		HFCL-ICpC		HFCL-SDT	
Passive	Active	Passive	Active	Passive	Active
$O(\frac{1}{t})$	$O(\frac{1}{t})$	$O(\frac{1}{t})$	$O(\frac{N^2}{t})$	$O(\frac{1}{\sqrt{Qt}+t})$	$O(\frac{1}{t})$

### A. Convergence Analysis

In this part, we analyze the convergence of the hybrid scenario, in which the convergence of the loss functions at the PS and the clients are investigated in the presence of corrupted model parameters. The convergence of ML models has been studied for both centralized [34] and federated [19, 29] schemes separately. Specifically, HFCL has the convergence rate of  $O(\frac{1}{t})$  as in CL and FL [19] while the performance of HFCL is subject to the noise in the model parameters as discussed in the previous section. We summarize the convergence rates of the proposed algorithms in Table II for both active and passive clients.

During model training, we make the following assumptions needed to ensure the convergence, which are typical for the  $l_2$ -norm regularized linear regression, logistic regression, and softmax classifiers [16, 19, 29].

*Assumption 1:* The loss function  $\mathcal{F}_k(\boldsymbol{\theta})$  is convex, i.e.,  $\mathcal{F}_k((1-\lambda)\boldsymbol{\theta} + \lambda\boldsymbol{\theta}') \leq (1-\lambda)\mathcal{F}_k(\boldsymbol{\theta}) + \lambda\mathcal{F}_k(\boldsymbol{\theta}')$  for  $\lambda \in [0, 1]$  and arbitrary  $\boldsymbol{\theta}$  and  $\boldsymbol{\theta}'$ .

*Assumption 2:*  $\mathcal{F}_k(\boldsymbol{\theta})$  is  $L$ -Lipschitz, i.e.,  $\|\mathcal{F}_k(\boldsymbol{\theta}) - \mathcal{F}_k(\boldsymbol{\theta}')\| \leq L\|\boldsymbol{\theta} - \boldsymbol{\theta}'\|$  for arbitrary  $\boldsymbol{\theta}$  and  $\boldsymbol{\theta}'$ .

*Assumption 3:*  $\mathcal{F}_k(\boldsymbol{\theta})$  is  $\beta$ -Smooth, i.e.,  $\|\nabla\mathcal{F}_k(\boldsymbol{\theta}) - \nabla\mathcal{F}_k(\boldsymbol{\theta}')\| \leq \beta\|\boldsymbol{\theta} - \boldsymbol{\theta}'\|$  for arbitrary  $\boldsymbol{\theta}$  and  $\boldsymbol{\theta}'$ .

In order to prove the convergence of the loss functions for passive and active clients, i.e.,  $\tilde{\mathcal{F}}_k(\boldsymbol{\theta})$  and  $\bar{\mathcal{F}}_k(\boldsymbol{\theta})$ , we first investigate the  $\beta$ -Smoothness of  $\bar{\mathcal{F}}_k(\boldsymbol{\theta})$  in the following lemma.

**Lemma 1.**  $\bar{\mathcal{F}}_k(\boldsymbol{\theta})$  is a  $\bar{\beta}$ -Smooth function with  $\|\nabla\bar{\mathcal{F}}_k(\boldsymbol{\theta}) - \nabla\bar{\mathcal{F}}_k(\boldsymbol{\theta}')\| \leq \bar{\beta}\|\boldsymbol{\theta} - \boldsymbol{\theta}'\|$ , where  $\bar{\beta} = (1 + \tilde{\sigma}^2 + \sigma_k^2)\beta$ .

*Proof:* See Appendix A. ■

Using Lemma 1 and (14), it is straightforward to show that  $\tilde{\mathcal{F}}_k(\boldsymbol{\theta})$  is a  $\bar{\beta}$ -smooth function with  $\bar{\beta} = \tilde{\sigma}^2\beta$ .

**Theorem 1.** At the  $k$ th active client ( $k \in \bar{\mathcal{L}}$ ), the loss function  $\tilde{\mathcal{F}}_k(\boldsymbol{\theta})$  satisfies

$$\tilde{\mathcal{F}}_k(\boldsymbol{\theta}^{(t)}) - \tilde{\mathcal{F}}_k(\boldsymbol{\theta}^*) \leq \|\boldsymbol{\theta}^{(0)} - \boldsymbol{\theta}^*\|^2 \frac{1}{2\eta t}, \quad (20)$$

with the learning rate  $\eta \leq \frac{1}{(1+\tilde{\sigma}^2+\sigma_k^2)\bar{\beta}}$  and  $\boldsymbol{\theta}^*$  is the minimizer of  $\tilde{\mathcal{F}}_k(\boldsymbol{\theta})$ .

*Proof:* See Appendix B. ■

Based on Theorem 1, the loss function of the passive clients  $\bar{\mathcal{F}}_k(\boldsymbol{\theta})$  is said to be convergent with

$$\bar{\mathcal{F}}_k(\boldsymbol{\theta}^{(t)}) - \bar{\mathcal{F}}_k(\boldsymbol{\theta}^*) \leq \|\boldsymbol{\theta}^{(0)} - \boldsymbol{\theta}^*\|^2 \frac{1}{2\eta t}, \quad (21)$$

with the learning rate  $\eta \leq \frac{1}{(1+\tilde{\sigma}^2)\bar{\beta}}$  since the problem for passive clients is corrupted by the noise  $\tilde{\Delta}\boldsymbol{\theta} = \frac{1}{D} \sum_{k \in \bar{\mathcal{L}}} D_k \Delta\boldsymbol{\theta}_k$  with variance  $\tilde{\sigma}^2$  as in (10).

Consequently, if all of the clients perform CL, i.e.,  $L = K$ , then we have  $\tilde{\sigma}^2 = \sigma_k^2 = 0$ . Conversely, if all of the clients perform FL, i.e.,  $L = 0$ , then the noise-free model parameters in (9) will vanish and the noise variance becomes  $\tilde{\sigma}_{\text{FL}}^2 = \frac{1}{D} \sum_{k \in \mathcal{K}} D_k \sigma_k^2$ . Thus, FL converges with lower learning performance than that of CL [16]. On the other hand, assuming  $D_1 = \dots = D_K$  and  $\sigma_1^2 = \dots = \sigma_K^2$ , the noise variance in HFCL  $\tilde{\sigma}_{\text{HFCL}}^2 = \frac{1}{D} \sum_{k \in \bar{\mathcal{L}}} D_k \sigma_k^2$  becomes less than  $\tilde{\sigma}_{\text{FL}}^2$  since  $\sum_{k \in \bar{\mathcal{L}}} \sigma_k^2 < \sum_{k \in \mathcal{K}} \sigma_k^2$ , where  $K - L < K$  for  $L \geq 1$ . Therefore, the performance of HFCL is upper- and lower bounded by CL and FL, respectively, as  $0 \leq \tilde{\sigma}_{\text{HFCL}}^2 \leq \tilde{\sigma}_{\text{FL}}^2$ .

*Remark 1:* If  $D_{k_1} \neq D_{k_2}$ , where  $k_1, k_2 \in \mathcal{K}$  and  $k_1 \neq k_2$ , then the performance of HFCL may be lower than FL. For instance, assume that  $\sigma_1^2 = \dots = \sigma_K^2$ , if  $\frac{1}{D} \sum_{k \in \bar{\mathcal{L}}} D_k > \frac{1}{D} \sum_{k \in \mathcal{K}} D_k$ , HFCL converges with higher noise than that of FL since  $\tilde{\sigma}_{\text{HFCL}}^2 > \tilde{\sigma}_{\text{FL}}^2$ . While the equality of  $\sigma_k^2 \in \mathcal{K}$  may be practical, the performance of HFCL and FL is subject to the size of the datasets [16, 19].

*Remark 2:* The choice of the learning rate  $\eta$  is important for the convergence of the learning algorithms, e.g., CL, FL and HFCL. Due to the effect of noisy learning parameters, FL and HFCL behave very differently than CL. Since the noise-related parameters, such as  $\tilde{\sigma}^2$  and  $\sigma_k^2$ , are unknown, the common choice is to employ a decaying learning rate, which can provide convergence to the optimum  $\boldsymbol{\theta}^*$  both in FL and HFCL [19, 32].

### B. Communication Overhead

The communication overhead is due to the transmission of dataset or the model parameters that are exchanged between the clients and the PS, wherein several signal processing techniques, such as channel acquisition, quantization and resource allocation, are employed. Hence, the communication overhead can be measured by the number of transmitted symbols during model training [8, 13, 21, 22]. Thus, the communication overhead of CL ( $\mathcal{T}_{\text{CL}}$ ) can be given by the number of symbols used to transmit datasets while the overhead during FL ( $\mathcal{T}_{\text{FL}}$ ) is proportional to the number of communication rounds  $T$  and model parameters  $P$ . Let  $\mathbf{D} = \sum_{k \in \mathcal{K}} \mathbf{d}_k$  be the number of symbols of the whole dataset, then the communication overhead of CL, FL and HFCL are given respectively as

$$\mathcal{T}_{\text{CL}} = \mathbf{D}, \quad (22)$$

$$\mathcal{T}_{\text{FL}} = 2TPK, \quad (23)$$

$$\mathcal{T}_{\text{HFCL}} = L\mathbf{d}_{k \in \bar{\mathcal{L}}} + 2TP(K - L), \quad (24)$$

where  $\mathcal{T}_{\text{HFCL}}$  includes the transmission of dataset of  $L$  passive clients and model parameters of  $K - L$  active clients. It is reasonable to assume that the size of the datasets is larger than the size of the model parameters, i.e.,  $\mathcal{T}_{\text{FL}} \leq \mathcal{T}_{\text{CL}}$  [8, 12, 13, 21, 22], then, we have  $\mathcal{T}_{\text{FL}} \leq \mathcal{T}_{\text{HFCL}} \leq \mathcal{T}_{\text{CL}}$ . Notice that the communication overhead is equal for all HFCL techniques proposed in this work, since they all involve the same amount of dataset and model transmission.

## VII. NUMERICAL SIMULATIONS

In this section, we present the performance of the proposed HFCL frameworks in comparison to traditional CL- and FL-based training. We evaluate the performance on two datasets:

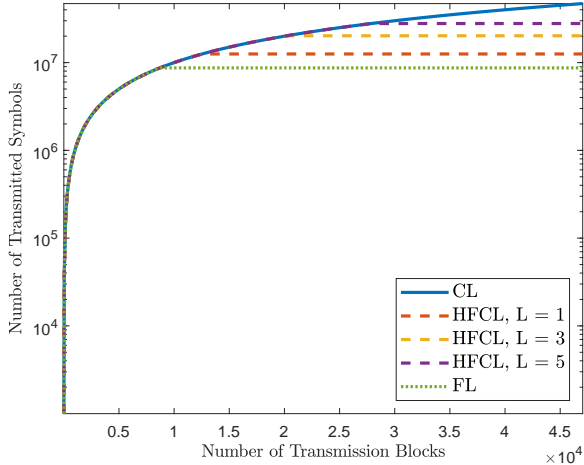


Fig. 2. Communication overhead comparison.

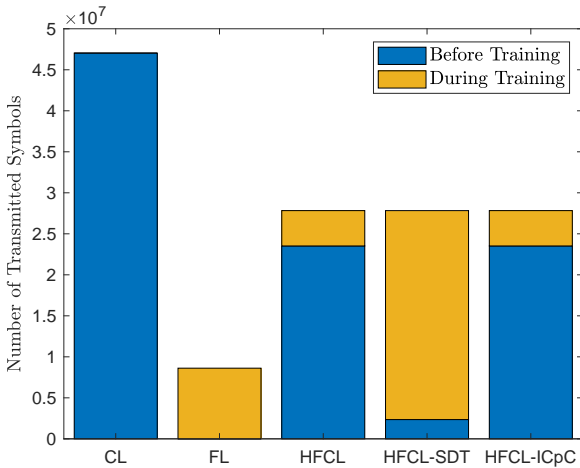


Fig. 3. Number of transmitted symbols before and during training when  $L = 5$ .

image classification on MNIST dataset [35] and 3D object detection on Lyft Level 5 AV dataset [36].

#### A. Image Classification

We evaluate the performance on MNIST dataset [35] including  $28 \times 28$  gray-scale images of handwritten digits with 10 classes. The number of symbols on the whole dataset is  $D = 28^2 \cdot 60,000 \approx 47 \times 10^6$ . During model training, the dataset is partitioned into  $K = 10$  blocks, each of which is available at the clients with identically independent distribution. Further, we train a CNN with 6 layers. The first layer is  $28 \times 28$  input layer. The second and the fourth layers are convolutional layers with  $5 \times 5 @ 128$  and  $3 \times 3 @ 128$  spatial filters, respectively. After each convolutional layer, there is a ReLU layer, which operates  $\max(0, x)$  for its input  $x$ . The output layer is a classification layer, which computes the probability distribution of the input data for 10 classes.

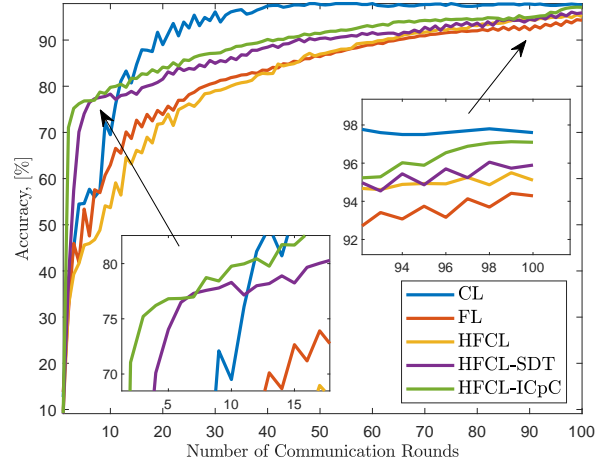


Fig. 4. Classification accuracy versus number communication rounds when  $L = 5$   $\text{SNR}_\theta = 20$  dB and  $B = 5$ .

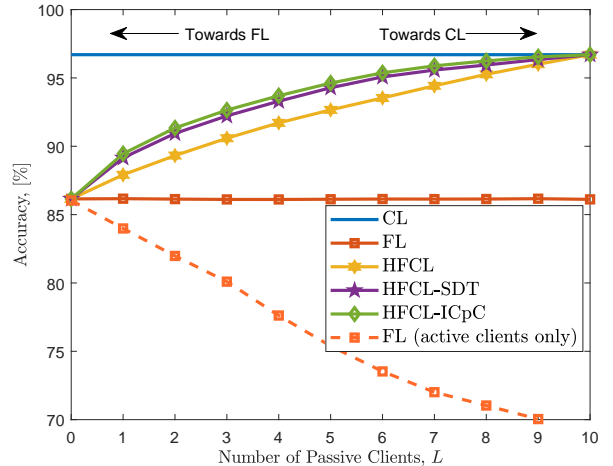


Fig. 5. Classification accuracy versus  $L$  when  $\text{SNR}_\theta = 20$  dB and  $B = 8$ .

Thus, we have  $P = 128 \cdot (5^2 + 3^2) = 4,352$  learnable parameters. The validation data of MNIST dataset include 10,000 images. The learning rate is selected as 0.001, which is reduced by half after each 30 iterations, and the mini-batch size is selected as 128 for CL. The loss function was the cross-entropy cost as  $-\frac{1}{D} \sum_{i=1}^D \sum_{c=1}^{\bar{C}} \left[ \mathcal{Y}_i^{(c)} \ln \hat{\mathcal{Y}}_i^{(c)} + (1 - \mathcal{Y}_i^{(c)}) \ln(1 - \hat{\mathcal{Y}}_i^{(c)}) \right]$ , where  $\{\mathcal{Y}_i^{(c)}, \hat{\mathcal{Y}}_i^{(c)}\}_{i=1, c=1}^{D, \bar{C}}$  is the true and predicted response for the classification layer with  $\bar{C} = 10$ . The classification accuracy is  $\text{Accuracy}(\%) = \frac{U}{D} \times 100$ , in which the model identified the image class correctly  $U$  times. Further, we define the SNR during model transmission as  $\text{SNR}_\theta = 20 \log_{10} \frac{\|\theta\|_2^2}{\sigma_\theta^2}$ , where  $\sigma_\theta^2 = \tilde{\sigma}^2 + \sigma_k^2$  denotes the total amount of noise variance during model transmission, for which we assume  $\sigma_{L+1}^2 = \dots = \sigma_K^2$  for simplicity.

Fig. 2 shows the communication overhead of CL, FL and



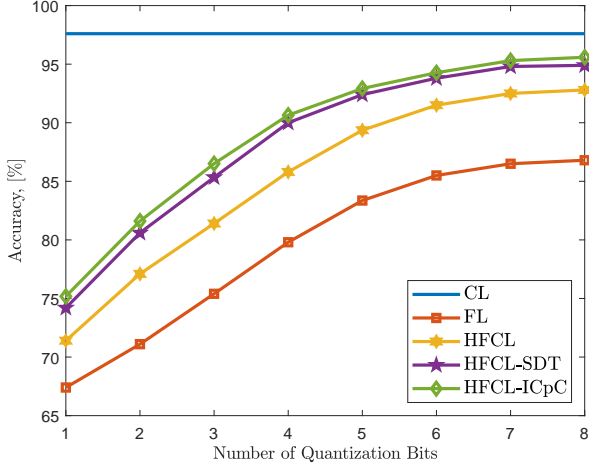


Fig. 6. Classification accuracy versus  $B$  when  $\text{SNR}_\theta = 20$  dB.

HFCL for  $L = \{0, 1, 3, 5, 7, 10\}$ . During model training, we assume that 1000 data symbols are transmitted at each transmission block. Thus, it takes approximately  $47 \times 10^3$  transmission blocks to complete CL-based training, while FL demands approximately  $8,5 \times 10^3$  data blocks, which are approximately 6 times lower than that of CL. The communication overhead of HFCL (as well as HFCL-SDT and HFCL-ICpC) is between CL and FL since it depends on the number of passive clients  $L$  and approaches to  $\mathcal{T}_{\text{CL}}$  as  $L \rightarrow K$ .

To explicitly present the overhead for the hybrid frameworks, the number of transmitted symbols before ( $t = 0$ ) and during ( $t > 0$ ) training is presented in Fig. 3. Specifically, the whole communication overhead of CL is at  $t = 0$  before training due the dataset transmission. In contrast, the overhead of FL is observed during training since no dataset transmission is involved, yet model transmission is taken place when  $t > 0$ . For the HFCL, they involve communication overheads before and during training since they involve both dataset and model transmission. Also, it is clear that the overhead of all hybrid frameworks are the same because they all involve the same amount of dataset and model transmission. However, they distinguish in terms of the number of symbols transmitted before and during training. While HFCL and HFCL-ICpC have the same amount of overhead during training, HFCL-SDT has lower overhead before training due to transmitting the datasets sequentially. Furthermore, we see that the overhead of FL is twice of the amount during training for HFCL and HFCL-ICpC. This is because  $L = 5$  for HFCL and HFCL-ICpC, and  $L = K = 10$  for FL. While the overhead of FL may seem lower compared to our HFCL frameworks, the former does not work if the clients have no capability for model computation, which is taken into account in the latter frameworks at the cost of a moderate increase in the overhead.

In Fig. 4, we present the training performance of the competing methods for  $L = 5$ ,  $\text{SNR}_\theta = 20$  dB and  $B = 5$  quantization bits. HFCL-ICpC has higher accuracy at the beginning of training due to multiple updates at the active

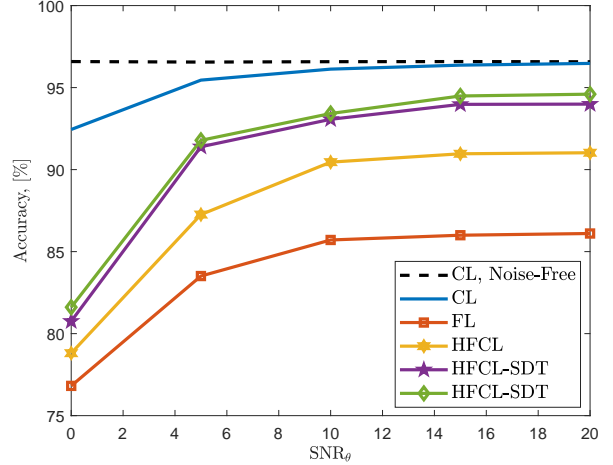


Fig. 7. Classification accuracy versus  $\text{SNR}_\theta$  when  $L = 5$  and  $B = 5$ .

clients, and it keeps outperforming HFCL and HFCL-SDT for the remaining iterations. Thanks to STD, HFCL-SDT also has higher performance than HFCL, which performs better than conventional FL. Notice that all the proposed HFCL approaches have moderate performance between FL and CL, as theoretically proved in Section VI. We note that the performance of FL is computed by assuming that all of  $K$  clients participate in training, which is not possible if there exist passive clients, for which FL is not the applicable training framework.

Fig. 5 shows the classification accuracy with respect to number of passive clients  $L$  when  $\text{SNR}_\theta = 20$  dB. The proposed HFCL approaches perform better than FL for  $0 < L < K$  since, in FL, the collected models from the active clients are corrupted by wireless channel whose effects reduce as  $L \rightarrow K$ . When  $L = 0$ , HFCL, HFCL-SDT and HFCL-ICpC are identical to FL since all the clients are active whereas they perform the same as CL if  $L = K = 10$  since all the clients are passive, i.e., they transmit their datasets to the PS and noise-free model parameters can be used for model training. Comparing the HFCL algorithms yields that both HFCL-ICpC and HFCL-SDT provide higher accuracy than HFCL for  $0 < L < K$ . HFCL-ICpC starts the training process when  $t = 0$  with locally-updated models at the active clients, thus, provides higher accuracy than both HFCL and HFCL-SDT. Also, HFCL-SDT starts the training with the same conditions as in HFCL while HFCL-SDT incorporates smaller datasets at the beginning for  $t < N$ , thus, reaching higher accuracy levels quicker than HFCL, which computes the model parameters on the whole local dataset of the passive clients for  $t < N$ , leading to a slower convergence rate.

In Fig. 5, we also present the performance of FL with active clients only, that is to say, the learning model is trained on only the dataset of active clients, whereas it is tested on the whole dataset. We observe that FL becomes unable to learn the data as  $L$  increases since the training is conducted only on the datasets of active clients. This shows the effectiveness of

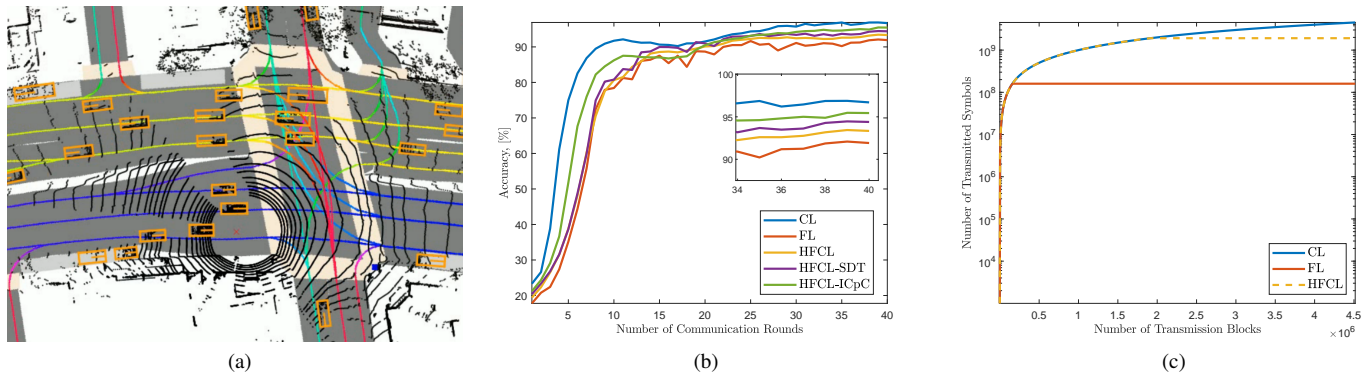


Fig. 8. 3D object detection. (a) Visualization of input and output data, (b) object detection performance and (c) communication overhead.

our HFCL approach, in which all of the clients participate the learning stage. It is worthwhile to note that when  $L = K = 10$ , there will be no active clients as FL with only active clients cannot work. The performance loss as  $L \rightarrow K$  is due to the absence of passive clients' datasets can be severe if the dataset is non-identically distributed because the active clients cannot learn the whole features in the dataset of other devices.

In Fig. 6, we present the classification accuracy with respect to the quantization level of the model parameters for  $B \in [1, 8]$  when  $\text{SNR}_\theta = 20$  dB. Note that quantization is only applied to wireless-transmitted models, i.e., FL and HFCL. Hence, the performance of CL does not change. The model parameters are quantized layer by layer between the maximum and minimum weights of each layer [15]. As expected, classification accuracy improves as  $B$  increases due to the enhancement of the model precision. We can conclude that at least 5 bit quantization is required for reliable classification accuracy.

We further present the classification performance with respect to the noise corruption on the transmitted information, i.e., the model parameters and the datasets. Fig. 7 shows the classification accuracy of the competing algorithms for  $\text{SNR}_\theta = [0, 20]$  dB and  $\text{SNR}_\theta = \text{SNR}_D$ , which is defined as the SNR of the noise added onto the transmitted datasets. We observe that at least 10 dB noise level is required for reliable model training for all approaches. Compared to the FL and the proposed hybrid algorithms, CL is more robust against noise since its model parameters are not corrupted by wireless transmission since they are computed at the PS. Comparing the effect of noise in datasets and model parameters, it can be concluded that the learning accuracy is more impacted by the corruptions in the model than the datasets. This is because the noise in the model makes it unable to learn the data while the noise in the dataset is, to some extent, helpful to make the model robust against the imperfections in the data. Therefore, artificial noise is usually added onto the dataset in many applications, such as image classification [2, 3], and physical layer design in wireless communications [15, 22].

### B. 3D Object Detection

We evaluate the performance of the HFCL framework on 3D object detection problem in vehicular networks, based on the Lyft Level 5 AV dataset [36], collected from lidar and

cameras mounted on vehicles [7]. The input data is selected as a top view image of the ego vehicle, which includes the received lidar signal strengths for different elevations, as shown in Fig. 8a. The output data is the classified representation of the vehicles/objects as boxes, which is obtained by the preprocessing of the images from the cameras, as illustrated in Fig. 8a<sup>3</sup>. The training dataset is collected from 10 vehicles in different areas after preprocessing of camera and lidar data. We assume  $L = 3$  of the vehicles are passive while the remaining ones are active clients. Each dataset includes  $10^3$  input-output pairs, whose sizes are  $336 \times 336 \times 3$  and  $336 \times 336 \times 1$ , respectively. Hence, the total number of data symbols is  $(336 \times 336 \times 3 + 336 \times 336) \times 10^4 \approx 4.5 \times 10^9$ . The dataset has 9 classes, i.e., car, motorcycle, bus, bicycle, truck, pedestrian, other vehicle, animal, emergency vehicle, which are represented by the boxes as shown in Fig. 8a. We have used U-net [37] with 8 convolutional layers to learn the features in the input data and achieve 3D object detection and segmentation. The total number of parameters in U-net is approximately  $2 \times 10^6$ , and training is conducted for  $T = 40$  communication rounds.

The training performance of the competing methods is presented in Fig. 8b, from which we obtain similar observations as in the image classification scenario in the previous part. HFCL methods provide a moderate performance between CL and FL. Nevertheless, all of the vehicles can participate in training while the conventional FL methods cannot support it and the communication overhead of CL is prohibitive. Thus, HFCL solves the trade-off on the computational capability of the clients and the communication overhead.

In Fig. 8c, number of transmitted data symbols for CL, FL and HFCL are presented. The overhead of CL is due to the transmission of whole data symbols, i.e., approximately  $4.5 \times 10^9$ . In contrast, the complexity of FL is due to the two way (edge  $\leftrightarrow$  server) transmission of the model updates during training until convergence, i.e.,  $2 \times 40 \times (2 \times 10^6) = 160 \times 10^6$  for 40 iterations. As a result, FL and HFCL have approximately 28 and 3 times lower communication overhead as compared to CL, respectively. The effectiveness of HFCL

<sup>3</sup>While we assumed that the dataset is labeled, the annotation of the objects in the data samples is an important task, for which the reader can refer to [7, 8].

in terms of overhead is reduced as compared to the image classification application because of larger input size of object detection problem (i.e.,  $336 \times 336 \times 3$  versus  $28 \times 28 \times 1$ ).

### VIII. SUMMARY

In this paper, we introduce a hybrid federated and centralized learning (HFCL) approach for distributed machine learning tasks. The proposed approach is helpful if a portion of the edge devices do not have the computational capability for model computation during training. In order to train the learning model collaboratively, only active devices, which have sufficient computational capability, perform FL by computing the model updates on their local datasets whereas the remaining passive devices, which do not have enough computational power, resort to CL and send their local datasets to the PS, which perform the model computation on behalf of them. As a result, HFCL solves the trade-off between FL and CL in terms of computation capability of edge devices and communication overhead. The transmission of local datasets may generate delays during training if the dataset size of the passive clients is large. This problem is mitigated by the proposed HFCL-ICpC and HFCL-SDT frameworks. While the former improves learning accuracy with more model computation-per-client, the latter reduces the size of the transmitted datasets. Compared to CL, the proposed approach is advantageous due to the reduction in the communication latency. In the meantime, compared to FL, a major drawback of the proposed HFCL approach is that HFCL requires the dataset transmission of the passive clients, which may raise privacy concerns, which are already apparent in CL. Nevertheless, HFCL provide access to the dataset of all devices regardless of their computational capability whereas, in FL, only the dataset of the passive clients could be used. We show that our HFCL approach has significant performance improvement as compared to FL-based training with only active clients since FL cannot access the dataset of all clients. As future work, we plan to study the application of HFCL to physical layer applications, such as channel estimation, resource allocation and beamforming.

#### APPENDIX A PROOF OF LEMMA 1

Using (12), we get

$$\begin{aligned}
& \|\nabla \bar{\mathcal{F}}_k(\boldsymbol{\theta}) - \nabla \bar{\mathcal{F}}_k(\boldsymbol{\theta}')\| \\
&= \|\nabla(\mathcal{F}_k(\boldsymbol{\theta}) + (\tilde{\sigma}^2 + \sigma_k^2)\|\nabla \mathcal{F}_k(\boldsymbol{\theta})\|^2) \\
&\quad - \nabla(\mathcal{F}_k(\boldsymbol{\theta}') + (\tilde{\sigma}^2 + \sigma_k^2)\|\nabla \mathcal{F}_k(\boldsymbol{\theta}')\|^2)\| \\
&= \|(\nabla \mathcal{F}_k(\boldsymbol{\theta}) + (\tilde{\sigma}^2 + \sigma_k^2)\nabla\|\nabla \mathcal{F}_k(\boldsymbol{\theta})\|^2) \\
&\quad - (\nabla \mathcal{F}_k(\boldsymbol{\theta}') + (\tilde{\sigma}^2 + \sigma_k^2)\nabla\|\nabla \mathcal{F}_k(\boldsymbol{\theta}')\|^2)\| \\
&= \|\nabla \mathcal{F}_k(\boldsymbol{\theta}) - \nabla \mathcal{F}_k(\boldsymbol{\theta}') + (\tilde{\sigma}^2 + \sigma_k^2) \\
&\quad \times (\nabla \text{tr}\{\nabla \mathcal{F}_k(\boldsymbol{\theta})^\top \nabla \mathcal{F}_k(\boldsymbol{\theta})\} - \nabla \text{tr}\{\nabla \mathcal{F}_k(\boldsymbol{\theta}')^\top \nabla \mathcal{F}_k(\boldsymbol{\theta}')\})\| \\
&= \|\nabla \mathcal{F}_k(\boldsymbol{\theta}) - \nabla \mathcal{F}_k(\boldsymbol{\theta}') \\
&\quad + (\tilde{\sigma}^2 + \sigma_k^2)(\nabla \mathcal{F}_k(\boldsymbol{\theta}) - \nabla \mathcal{F}_k(\boldsymbol{\theta}')\|\| \\
&= \|(1 + \tilde{\sigma}^2 + \sigma_k^2)(\nabla \mathcal{F}_k(\boldsymbol{\theta}) - \nabla \mathcal{F}_k(\boldsymbol{\theta}')\|\| \\
&= (1 + \tilde{\sigma}^2 + \sigma_k^2)\|\nabla \mathcal{F}_k(\boldsymbol{\theta}) - \nabla \mathcal{F}_k(\boldsymbol{\theta}')\|. \tag{25}
\end{aligned}$$

By incorporating (25), Assumption 2 and the fact that  $1 + (\tilde{\sigma}^2 + \sigma_k^2) \geq 0$ , we get

$$\|\nabla \bar{\mathcal{F}}_k(\boldsymbol{\theta}) - \nabla \bar{\mathcal{F}}_k(\boldsymbol{\theta}')\| \leq \tilde{\beta} \|\boldsymbol{\theta} - \boldsymbol{\theta}'\|^2, \tag{26}$$

where  $\tilde{\beta} = (1 + (\tilde{\sigma}^2 + \sigma_k^2))\beta$ .

#### APPENDIX B PROOF OF THEOREM 1

Using (26), Assumption 2 and Assumption 3 imply that  $\bar{\mathcal{F}}_k(\boldsymbol{\theta})$  is second order differentiable as  $\nabla^2 \bar{\mathcal{F}}_k(\boldsymbol{\theta}) \preceq \tilde{\beta} \mathbf{I}_P$ . Using this fact, performing a quadratic expression around  $\bar{\mathcal{F}}_k(\boldsymbol{\theta})$  yields

$$\begin{aligned}
\bar{\mathcal{F}}_k(\boldsymbol{\theta}') &\leq \bar{\mathcal{F}}_k(\boldsymbol{\theta}) + \nabla \bar{\mathcal{F}}_k(\boldsymbol{\theta})^\top (\boldsymbol{\theta}' - \boldsymbol{\theta}) + \frac{1}{2} \nabla^2 \bar{\mathcal{F}}_k(\boldsymbol{\theta}) \|\boldsymbol{\theta}' - \boldsymbol{\theta}\|^2 \\
&\leq \mathcal{F}_k(\boldsymbol{\theta}) + \nabla \bar{\mathcal{F}}_k(\boldsymbol{\theta})^\top (\boldsymbol{\theta}' - \boldsymbol{\theta}) + \frac{1}{2} \tilde{\beta} \|\boldsymbol{\theta}' - \boldsymbol{\theta}\|^2. \tag{27}
\end{aligned}$$

Substituting the GD update  $\boldsymbol{\theta}' = \boldsymbol{\theta} - \eta \nabla \bar{\mathcal{F}}_k(\boldsymbol{\theta})$  in (27), we get

$$\begin{aligned}
\bar{\mathcal{F}}_k(\boldsymbol{\theta}') &\leq \bar{\mathcal{F}}_k(\boldsymbol{\theta}) + \nabla \bar{\mathcal{F}}_k(\boldsymbol{\theta})^\top (\boldsymbol{\theta}' - \boldsymbol{\theta}) + \frac{1}{2} \tilde{\beta} \|\boldsymbol{\theta}' - \boldsymbol{\theta}\|^2 \\
&= \bar{\mathcal{F}}_k(\boldsymbol{\theta}) + \nabla \bar{\mathcal{F}}_k(\boldsymbol{\theta})^\top (\boldsymbol{\theta} - \eta \nabla \bar{\mathcal{F}}_k(\boldsymbol{\theta}) - \boldsymbol{\theta}) \\
&\quad + \frac{1}{2} \nabla^2 \bar{\mathcal{F}}_k(\boldsymbol{\theta}) \|\boldsymbol{\theta} - \eta \nabla \bar{\mathcal{F}}_k(\boldsymbol{\theta}) - \boldsymbol{\theta}\|^2 \\
&= \bar{\mathcal{F}}_k(\boldsymbol{\theta}) - \eta \nabla \bar{\mathcal{F}}_k(\boldsymbol{\theta})^\top \nabla \bar{\mathcal{F}}_k(\boldsymbol{\theta}) + \frac{1}{2} \tilde{\beta} \|\eta \nabla \bar{\mathcal{F}}_k(\boldsymbol{\theta})\|^2 \\
&= \bar{\mathcal{F}}_k(\boldsymbol{\theta}) - \eta \|\nabla \bar{\mathcal{F}}_k(\boldsymbol{\theta})\|^2 + \frac{1}{2} \tilde{\beta} \eta^2 \|\nabla \bar{\mathcal{F}}_k(\boldsymbol{\theta})\|^2 \\
&= \bar{\mathcal{F}}_k(\boldsymbol{\theta}) - (1 - \frac{\tilde{\beta} \eta}{2}) \eta \|\nabla \bar{\mathcal{F}}_k(\boldsymbol{\theta})\|^2, \tag{28}
\end{aligned}$$

which bounds the GD update  $\bar{\mathcal{F}}_k(\boldsymbol{\theta}')$  with  $\bar{\mathcal{F}}_k(\boldsymbol{\theta})$ . Now, let us bound  $\bar{\mathcal{F}}_k(\boldsymbol{\theta}')$  with the optimal objective value  $\bar{\mathcal{F}}_k(\boldsymbol{\theta}^*)$ . Using Assumption 1, we have

$$\begin{aligned}
\bar{\mathcal{F}}_k(\boldsymbol{\theta}^*) &\geq \bar{\mathcal{F}}_k(\boldsymbol{\theta}) + \nabla \bar{\mathcal{F}}_k(\boldsymbol{\theta})^\top (\boldsymbol{\theta}^* - \boldsymbol{\theta}), \\
\bar{\mathcal{F}}_k(\boldsymbol{\theta}) &\leq \bar{\mathcal{F}}_k(\boldsymbol{\theta}^*) + \nabla \bar{\mathcal{F}}_k(\boldsymbol{\theta})^\top (\boldsymbol{\theta} - \boldsymbol{\theta}^*). \tag{29}
\end{aligned}$$

Furthermore, using  $\eta \leq \frac{1}{\tilde{\beta}}$ , we have  $-(1 - \frac{\tilde{\beta} \eta}{2}) = \frac{1}{2} \tilde{\beta} \eta - 1 \leq \frac{1}{2} \tilde{\beta} (1/\tilde{\beta}) - 1 = \frac{1}{2} - 1 = -\frac{1}{2}$ . Thus, (28) becomes

$$\bar{\mathcal{F}}_k(\boldsymbol{\theta}') \leq \bar{\mathcal{F}}_k(\boldsymbol{\theta}) - \frac{\eta}{2} \|\nabla \bar{\mathcal{F}}_k(\boldsymbol{\theta})\|^2 \tag{30}$$

By plugging (29) into (30), we get

$$\bar{\mathcal{F}}_k(\boldsymbol{\theta}') \leq \bar{\mathcal{F}}_k(\boldsymbol{\theta}^*) + \nabla \bar{\mathcal{F}}_k(\boldsymbol{\theta})^\top (\boldsymbol{\theta} - \boldsymbol{\theta}^*) - \frac{\eta}{2} \|\nabla \bar{\mathcal{F}}_k(\boldsymbol{\theta})\|^2, \tag{31}$$

which can be rewritten as

$$\bar{\mathcal{F}}_k(\boldsymbol{\theta}') - \bar{\mathcal{F}}_k(\boldsymbol{\theta}^*) \leq \frac{1}{2\eta} \left( 2\eta \nabla \bar{\mathcal{F}}_k(\boldsymbol{\theta})^\top (\boldsymbol{\theta} - \boldsymbol{\theta}^*) - \eta^2 \|\nabla \bar{\mathcal{F}}_k(\boldsymbol{\theta})\|^2 \right). \tag{32}$$

By adding  $\frac{1}{2\eta} (\|\boldsymbol{\theta} - \boldsymbol{\theta}^*\|^2 - \|\boldsymbol{\theta} - \boldsymbol{\theta}^*\|^2)$  into the right hand side of (32), we get

$$\bar{\mathcal{F}}_k(\boldsymbol{\theta}') - \bar{\mathcal{F}}_k(\boldsymbol{\theta}^*) \leq \frac{1}{2\eta} \left( \|\boldsymbol{\theta} - \boldsymbol{\theta}^*\|^2 - \|\boldsymbol{\theta} - \boldsymbol{\theta}^* - \eta \nabla \bar{\mathcal{F}}_k(\boldsymbol{\theta})\|^2 \right), \tag{33}$$

which is obtained after incorporating the expansion of  $\|\theta - \theta^* - \eta \nabla \bar{\mathcal{F}}_k(\theta)\|^2$ . Substituting the GD update  $\theta' = \theta - \eta \nabla \bar{\mathcal{F}}_k(\theta)$  into (33), we have

$$\bar{\mathcal{F}}_k(\theta') - \bar{\mathcal{F}}_k(\theta^*) \leq \frac{1}{2\eta} \left( \|\theta - \theta^*\|^2 - \|\theta' - \theta^*\|^2 \right). \quad (34)$$

Now, let us replace  $\theta'$  with  $\theta^{(i)}$ , then summing over  $i = 1, \dots, t$  yields

$$\begin{aligned} & \sum_{i=1}^t (\bar{\mathcal{F}}_k(\theta^{(i)}) - \bar{\mathcal{F}}_k(\theta^*)) \\ & \leq \sum_{i=1}^t \frac{1}{2\eta} \left( \|\theta^{(i-1)} - \theta^*\|^2 - \|\theta^{(i)} - \theta^*\|^2 \right) \\ & = \frac{1}{2\eta} \left( \|\theta^{(0)} - \theta^*\|^2 - \|\theta^{(t)} - \theta^*\|^2 \right) \\ & \leq \frac{1}{2\eta} \|\theta^{(0)} - \theta^*\|^2, \end{aligned} \quad (35)$$

where the summation on the right hand side disappears since the consecutive terms cancel each other. Since  $\bar{\mathcal{F}}_k(\theta^{(t)})$  is a decreasing function, we have

$$\bar{\mathcal{F}}_k(\theta^{(t)}) - \bar{\mathcal{F}}_k(\theta^*) \leq \frac{1}{t} \sum_{i=1}^t (\bar{\mathcal{F}}_k(\theta^{(i)}) - \bar{\mathcal{F}}_k(\theta^*)). \quad (36)$$

Inserting (35) into (36), we finally have

$$\bar{\mathcal{F}}_k(\theta^{(t)}) - \bar{\mathcal{F}}_k(\theta^*) \leq \frac{1}{2\eta t} \|\theta^{(0)} - \theta^*\|^2. \quad (37)$$

## REFERENCES

- [1] A. M. Elbir, S. Coleri, and K. V. Mishra, "2021 29th European Signal Processing Conference (EUSIPCO)," 2002, Nov 2020. [Online]. Available: <https://arxiv.org/abs/2011.06892v2>
- [2] Y. Lecun, Y. Bengio, and G. Hinton, "Deep learning," *Nature*, vol. 521, no. 7553, pp. 436–444, 2015.
- [3] R. Mayer and H.-A. Jacobsen, "Scalable Deep Learning on Distributed Infrastructures: Challenges, Techniques, and Tools," *ACM Comput. Surv.*, vol. 53, no. 1, pp. 1–37, Feb 2020.
- [4] ITU-R, "Report ITU-R M.2370-0 (07/2015) IMT traffic estimates for the years 2020 to 2030," [https://www.itu.int/dms\\_pub/itu-r/otpb/rep/R-REP-M.2370-2015-PDF-E.pdf](https://www.itu.int/dms_pub/itu-r/otpb/rep/R-REP-M.2370-2015-PDF-E.pdf), [Online] Accessed: 2020-12-30.
- [5] H. Ye, L. Liang, G. Ye Li, J. Kim, L. Lu, and M. Wu, "Machine Learning for Vehicular Networks: Recent Advances and Application Examples," *IEEE Veh. Technol. Mag.*, vol. 13, no. 2, pp. 94–101, 2018.
- [6] "Machine learning for internet of things data analysis: a survey," *Digital Communications and Networks*, vol. 4, no. 3, pp. 161 – 175, 2018.
- [7] A. M. Elbir, B. Soner, and S. Coleri, "Federated Learning in Vehicular Networks," *arXiv*, Jun 2020. [Online]. Available: <https://arxiv.org/abs/2006.01412v2>
- [8] A. M. Elbir and K. V. Mishra, "Cognitive Learning-Aided Multi-Antenna Communications," *arXiv preprint arXiv:2010.03131*, 2020.
- [9] A. M. Elbir and K. V. Mishra, "A Survey of Deep Learning Architectures for Intelligent Reflecting Surfaces," *arXiv*, Sep 2020. [Online]. Available: <https://arxiv.org/abs/2009.02540v2>
- [10] O. Simeone, "A Very Brief Introduction to Machine Learning With Applications to Communication Systems," *IEEE Transactions on Cognitive Communications and Networking*, vol. 4, no. 4, pp. 648–664, Dec 2018.
- [11] J. Park, S. Samarakoon, M. Bennis, and M. Debbah, "Wireless Network Intelligence at the Edge," *Proc. IEEE*, vol. 107, no. 11, pp. 2204–2239, Nov 2019.
- [12] T. Li, A. K. Sahu, A. Talwalkar, and V. Smith, "Federated Learning: Challenges, Methods, and Future Directions," *IEEE Signal Process. Mag.*, vol. 37, no. 3, pp. 50–60, 2020.
- [13] M. Mohammadi Amiri and D. Gündüz, "Machine learning at the wireless edge: Distributed stochastic gradient descent over-the-air," *IEEE Trans. Signal Process.*, vol. 68, pp. 2155–2169, 2020.
- [14] M. M. Amiri and D. Gündüz, "Federated Learning Over Wireless Fading Channels," *IEEE Trans. Wireless Commun.*, vol. 19, no. 5, pp. 3546–3557, 2020.
- [15] A. M. Elbir and K. V. Mishra, "Joint antenna selection and hybrid beamformer design using unquantized and quantized deep learning networks," *IEEE Trans. Wireless Commun.*, vol. 19, no. 3, pp. 1677–1688, March 2020.
- [16] H. B. McMahan, E. Moore, D. Ramage, S. Hampson, and B. A. y. Arcas, "Communication-Efficient Learning of Deep Networks from Decentralized Data," *arXiv*, Feb 2016. [Online]. Available: <https://arxiv.org/abs/1602.05629v3>
- [17] Q. Yang, Y. Liu, T. Chen, and Y. Tong, "Federated Machine Learning: Concept and Applications," *ACM Trans. Intell. Syst. Technol.*, vol. 10, no. 2, pp. 1–19, Jan 2019.
- [18] K. Yang, T. Jiang, Y. Shi, and Z. Ding, "Federated learning via over-the-air computation," *IEEE Trans. Wireless Commun.*, vol. 19, no. 3, pp. 2022–2035, 2020.
- [19] X. Li, K. Huang, W. Yang, S. Wang, and Z. Zhang, "On the Convergence of FedAvg on Non-IID Data," in *International Conference on Learning Representations*, 2020. [Online]. Available: <https://openreview.net/forum?id=HJxNAnVtDS>
- [20] D. Guliani, F. Beaufays, and G. Motta, "Training Speech Recognition Models with Federated Learning: A Quality/Cost Framework," *arXiv*, Oct 2020. [Online]. Available: <https://arxiv.org/abs/2010.15965v1>
- [21] A. M. Elbir and S. Coleri, "Federated Learning for Hybrid Beamforming in mm-Wave Massive MIMO," *IEEE Commun. Lett.*, vol. 24, no. 12, pp. 2795–2799, Aug 2020.
- [22] A. M. Elbir and S. Coleri, "Federated Learning for Channel Estimation in Conventional and IRS-Assisted Massive MIMO," *arXiv preprint arXiv:2008.10846*, 2020.
- [23] D. Ma, L. Li, H. Ren, D. Wang, X. Li, and Z. Han, "Distributed Rate Optimization for Intelligent Reflecting Surface with Federated Learning," in *2020 IEEE International Conference on Communications Workshops (ICC Workshops)*, 2020, pp. 1–6.
- [24] M. M. Wadu, S. Samarakoon, and M. Bennis, "Federated learning under channel uncertainty: Joint client scheduling and resource allocation," *arXiv preprint arXiv:2002.00802*, 2020.
- [25] T. Zeng, O. Semiari, M. Mozaffari, M. Chen, W. Saad, and M. Bennis, "Federated Learning in the Sky: Joint Power Allocation and Scheduling with UAV Swarms," *arXiv preprint arXiv:2002.08196*, 2020.
- [26] L. U. Khan, W. Saad, Z. Han, E. Hossain, and C. S. Hong, "Federated Learning for Internet of Things: Recent Advances, Taxonomy, and Open Challenges," *arXiv*, Sep 2020. [Online]. Available: <https://arxiv.org/abs/2009.13012v1>
- [27] D. Ye, R. Yu, M. Pan, and Z. Han, "Federated learning in vehicular edge computing: A selective model aggregation approach," *IEEE Access*, vol. 8, pp. 23 920–23 935, 2020.
- [28] T. Nishio and R. Yonetani, "Client Selection for Federated Learning with Heterogeneous Resources in Mobile Edge," in *ICC 2019 - 2019 IEEE International Conference on Communications (ICC)*, 2019, pp. 1–7.
- [29] F. Ang, L. Chen, N. Zhao, Y. Chen, W. Wang, and F. R. Yu, "Robust Federated Learning With Noisy Communication," *IEEE Trans. Commun.*, vol. 68, no. 6, pp. 3452–3464, Mar 2020.
- [30] C. M. Bishop, "Training with Noise is Equivalent to Tikhonov Regularization," *Neural Comput.*, vol. 7, no. 1, pp. 108–116, Jan 1995.
- [31] S. Luo, X. Chen, Q. Wu, Z. Zhou, and S. Yu, "HFEL: Joint Edge Association and Resource Allocation for Cost-Efficient Hierarchical Federated Edge Learning," *arXiv*, Feb 2020. [Online]. Available: <https://arxiv.org/abs/2002.11343v2>
- [32] F. Haddadpour and M. Mahdavi, "On the Convergence of Local Descent Methods in Federated Learning," *arXiv*, Oct 2019. [Online]. Available: <https://arxiv.org/abs/1910.14425v2>
- [33] M. Li, T. Zhang, Y. Chen, and A. J. Smola, *Efficient mini-batch training for stochastic optimization*. New York, NY, USA: Association for Computing Machinery, Aug 2014.
- [34] S. Sra, S. Nowozin, and S. J. Wright, *Optimization for Machine Learning*. Cambridge, MA, USA: The MIT Press, Sep 2011.
- [35] Y. LeCun, C. Cortes, and C. Burges, "MNIST handwritten digit database," *ATT Labs [Online]*. Available: <http://yann.lecun.com/exdb/mnist>, vol. 2, 2010.
- [36] R. Kesten, M. Usman, J. Houston, T. Pandya, K. Nadhamuni, A. Ferreira, M. Yuan, B. Low, A. Jain, P. Ondruska, S. Omari, S. Shah, A. Kulkarni, A. Kazakova, C. Tao, L. Platinsky, W. Jiang, and V. Shet, "Lyft Level 5 AV Dataset 2019," 2019; <https://level5.lyft.com/dataset/>, accessed 1 Jun 2020.

- [37] O. Ronneberger, P. Fischer, and T. Brox, "U-net: Convolutional networks for biomedical image segmentation," in *International Conference on Medical image computing and computer-assisted intervention*. Springer, 2015, pp. 234–241.